X-RAY MICROTOMOGRAPHIC IMAGING OF KINK BANDS IN CARBON FIBRE-EPOXY COMPOSITES

Y. Wang[1*], C. Soutis[2], P. J. Withers[3]

[1]*Northwest Composites Centre, School of Materials, University of Manchester, Manchester, M13 9PL, UK*
[2]*Aerospace Research Institute, University of Manchester, Manchester, M13 9PL, UK*
[3]*Manchester X-ray Imaging Facility, School of Materials, University of Manchester, Manchester, M13 9PL, UK*
** ying.wang-13@postgrad.manchester.ac.uk*

Keywords: X-ray computed tomography (CT), fibre-reinforced composites, fibre micro-buckling, fibre kinking

Abstract
The three-dimensional (3-D) morphology of damage modes in kink bands formed in carbon fibre reinforced polymer (CFRP) composites under compression is presented. Specimens comprised unidirectional (UD) cylindrical carbon fibre/epoxy composite samples, fabricated using a small-scale resin infusion (SSRI) method. High-resolution X-ray micro-tomography (μCT), following uniaxial compression testing, has been used to visualise the morphology of kink bands and the associated failure mechanisms in 3-D. 3-D segmented volume and two-dimensional (2-D) orthogonal virtual sections parallel to the loading axis are used to help explain the kink band geometry, including the interaction between fully developed kink-band boundaries (defined by fibre breaks) and splitting along the fibre direction. It is proposed that two narrow bands formed at the points of maximum deflection caused the development of the wide kink band that leads to the final failure.

1. Introduction

Compressive failure of CFRP composite tends to be instantaneous and catastrophic due to the formation of fibre kink bands [1]. Four major failure mechanisms can occur: fibre micro-buckling, fibre kinking, fibre failure and splitting [2]. The cooperative interaction of these damage modes can lower the compressive strength of UD CFRP materials to 60-70% of their tensile strength [1-6]. Therefore, the prediction of compressive strength has always been of great interest in the effort to design more reliable CFRP composite structures [7, 8]. The understanding of geometric correlation between the failure mechanisms is essential for helping the development of strength-predicting models that can lead to more efficient aircraft designs.

The formation of kink bands has been investigated extensively experimentally in 2-D [3-6]. Fibre micro-buckling can be described as a micro-scale structural instability, while fibre kinking is associated with large matrix shear deformation induced by fibre micro-buckling which is affected by initial fibre waviness [9, 10]. The final abrupt failure results from fully-developed kink bands with fibre fracture and matrix failure. The important geometric

parameters relating to kink bands are illustrated in Fig. 1a, including the kink-band width ω, the kink-band angle β, and the angle of fibre rotation within the kink bands $\varphi+\varphi_o$ (φ_o is the initial fibre misalignment angle). Previously, the extent of the kinking region has been found to vary from 70µm to 800µm, with a constant width of individual kink bands at 60-100µm [5, 8]. These parameters not only depend on the material system (according to matrix shear modulus, initial fibre waviness, etc.), but also change during the failure process. In addition, these geometric parameters can be dependent on the cross section studied.

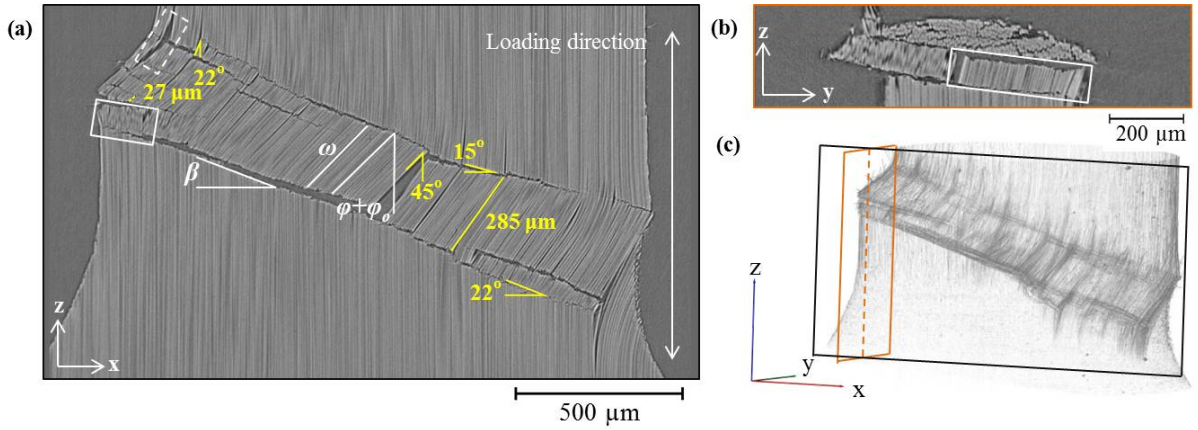

Figure 1. (a) Virtual tomographic XZ slice demonstrating the definitions and typical values of the geometric parameters of the kink bands for the sample studied in the present work (kink propagated approximately in the X direction), (b) orthogonal virtual tomographic YZ slice, and (c) volume rendering of the scanned specimen indicating the location of the section shown in (b).

In an effort to investigate the micromechanics of kink band formation, both post-mortem and *in-situ* characterisation using a combination of optical microscopy and scanning electron microscopy (SEM) have been previously undertaken [3-6]. Post-failure cross-sections cut so as to include the fibre direction have been carefully examined revealing the 2-D geometry of the kink bands, exhibiting single kink bands with or without fibre fractures at the boundaries, multiple kink bands and in-plane or out-of-plane kink bands. Unfortunately these techniques are destructive in nature and only provide a 2-D view of the microstructure. Meanwhile, as can be seen in Fig. 1c these failure mechanisms interact with each other in three dimensions, so that their observation using conventional techniques is not being truly representative of the deformed morphology. While non-destructive X-ray tomography has been applied to image the tensile failure [11] and impact damage [12] in CFRP composites, the analysis of compressive failure has not been reported. Here we used X-ray µCT to reveal the 3-D geometry of the kink bands and the interactions between the observed damage mechanisms (splitting and fibre failure).

Previously, the application of µCT in CFRP composites has met problems with low contrast between fibre and matrix, imaging challenges presented by high aspect ratio laminates, and limited field of view at sufficient resolution [13]. The contrast between carbon fibres and epoxy resin is very low because of their similar linear attenuation coefficients, making the imaging and segmentation of individual fibres difficult. Most of the research work to date studying kink bands has employed notched UD laminates having a relatively large width to thickness ratio [3-6]. The notches acted as stress risers to define the location of kink bands and also to slow the propagation of kink bands. From an X-ray imaging viewpoint the high aspect ratio would limit penetration of the X-rays, which can lead to artefacts. In other early experiments, cylindrical rod specimens confined by hydrostatic pressure have been used [14,

15]. Couque *et al.* [16] used a modified rod sample with a wasted gauge section, so as to constrain the kink band to initiate within the gauge length under hydrostatically confined compression. A novel testing method for pultruded cylindrical rods without lateral confinement has been proposed by Soutis [17].

The aim of the present study is to map the 3-D failure pattern of the kink bands developed under compression. Small-diameter cylindrical composite rods were fabricated using a SSRI method. X-ray μCT has then been used to image the specimen after compressive failure so as to visualise the kink bands in 3-D.

2. Experimental

2.1. Materials and sample preparation

UD composite rod samples were fabricated from Torayca T700 carbon fibre yarns and Huntsman Araldite LY 564/XB 3486 epoxy resin using a SSRI method, which was adapted from a conventional resin infusion process used to manufacture large panels. Instead of vacuum bagging, UD carbon fibre yarns were inserted into a 2.4mm glass tubes coated with release agent on the inner surface, as shown schematically in Fig. 2.

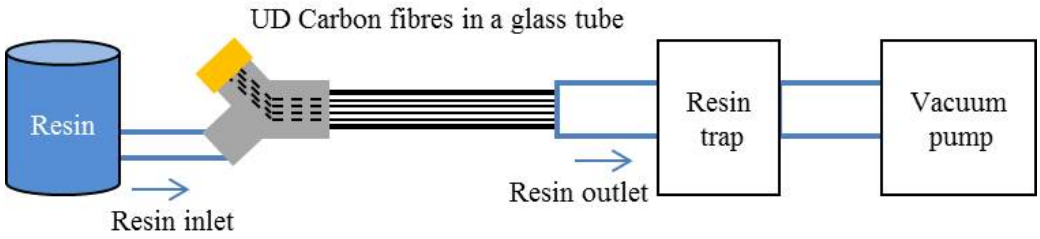

Figure 2. Schematic of the SSRI manufacturing method developed to make UD rods.

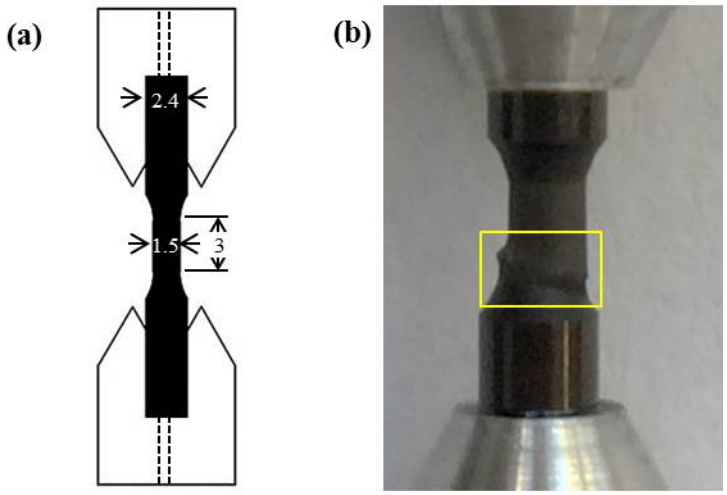

Figure 3. (a) Schematic of the specimen compression test geometry (dimensions in mm) with black representing the carbon fibre/epoxy rod and white the aluminium tabs, and (b) photograph of the specimen after failure, with the rectangular box indicating the region imaged by μCT.

In the uniaxial compression study of CFRP rods by Couque *et al.* [16], the specimens with a reduced gauge section were inserted in chamfered steel bases to a snug fit. For better load transfer, the specimen geometry in the current study, schematically shown in Fig. 3a, was

modified from that used by Couque *et al*. The two ends of the specimen were stuck with an epoxy adhesive into chamfered aluminium end caps having small holes drilled to remove and surplus epoxy. The middle section was ground down to a diameter of around 1.5mm over a 3mm long gauge, with smooth radii at the transition regions.

2.2. Compression testing and damage evaluation

Axial compressive end loading was applied to the specimens via the platens of a screw-driven test machine (Instron 5569) under a constant displacement rate of 0.02mm/min. Failed specimens were scanned on an Xradia 150kV MicroXCT in the Henry Moseley X-ray Imaging Facility with a voxel size of 1.1µm. A source voltage of 40 kV was used at a power of 10W. 1001 images (projections) were taken over a rotation of 180°, and the exposure time for each projection was 40 seconds. The Feldkamp-Davis-Kress (FDK) algorithm [18] was used for reconstruction and the reconstructed volume was analysed using Avizo (FEI Visualisation Sciences Group) visualisation software. Cracks were segmented according to the intensity values by using a local threshold function together with brushing within a limited intensity range. Interpolation was used on every ten slices and the 3-D segmentation was confirmed to be in accord with 2-D orthogonal slices.

3. Results and Discussion

3.1. Kink-band geometry

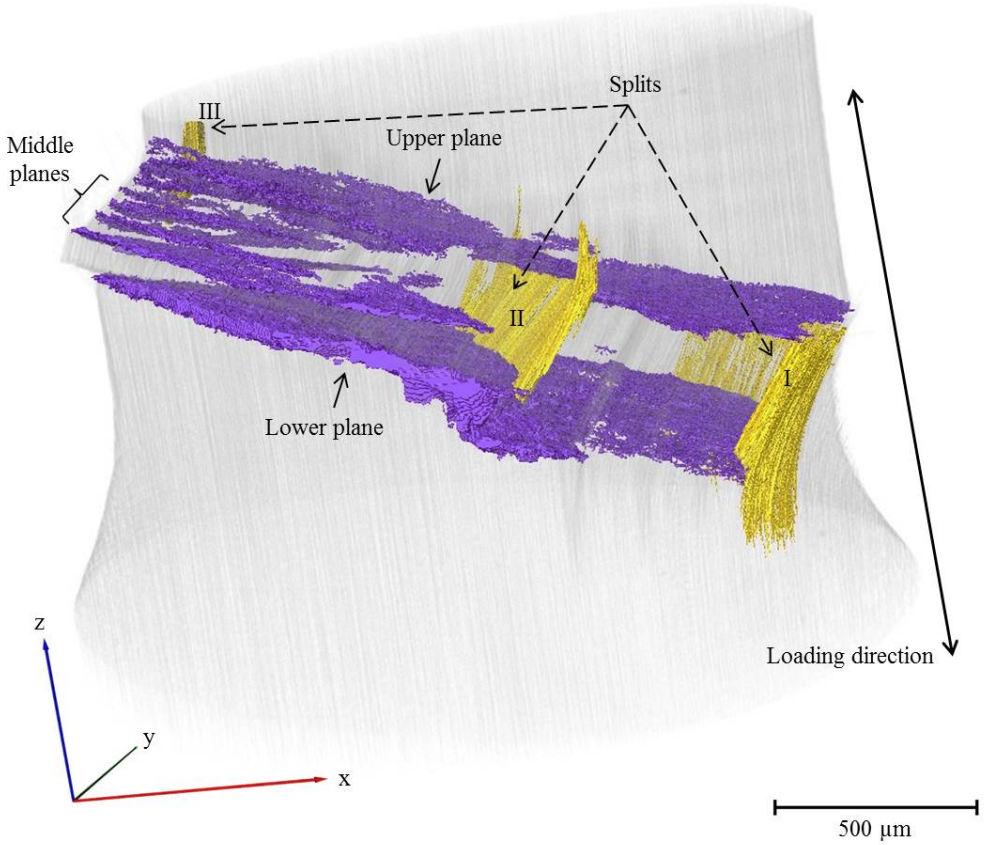

Figure 4. Side view of the segmented X-ray µCT image showing planes of fibre breakage (purple) normal to, and three splits (yellow) parallel to, the fibre direction. The upper and lower fibre-fracture planes delineate a wide kink band, within which multiple narrow bands that are similarly inclined lie.

After failure, a kink zone could be observed on the specimen surface as shown in Fig. 3b, located near the end of the gauge section possibly due to local stress concentration. Most of the specimens broke into two parts while being removed from the testing machine, which was not ideal for X-ray μCT scanning. The specimen discussed here is a representative one of the unseparated specimens. Fig. 4 exhibits processed μCT data of the kinked region highlighted in the yellow box in Fig. 3b. All the kink-band boundaries and three representative splits along the fibre direction were segmented and visualised. The geometric parameters of the kink bands are: ω = 20-320μm, β = 11-40°, $\varphi+\varphi_o$ = 18-52°.

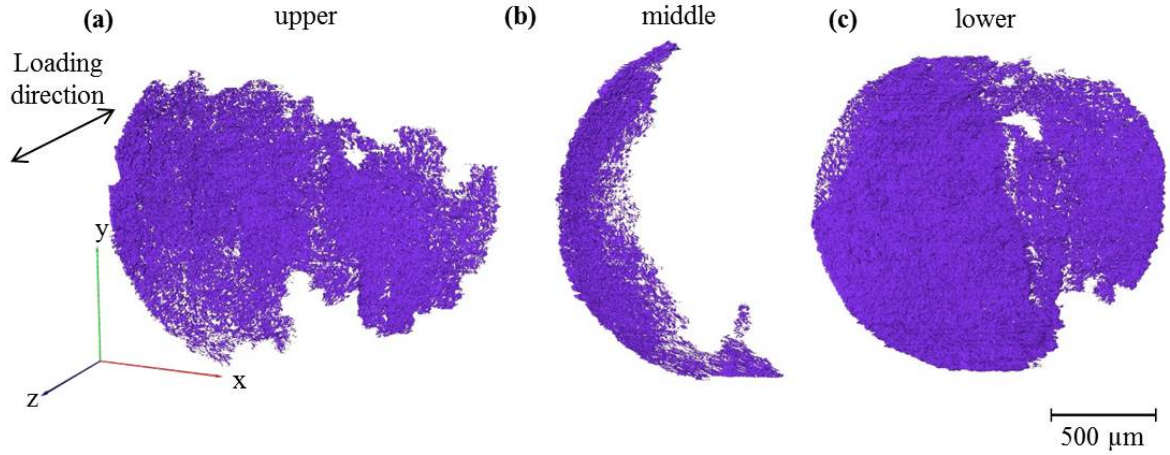

Figure 5. Top view of the segmented kink-band boundaries defined by fibre breakage, categorised in three groups according to their location and morphology: (a) upper, (b) middle and (c) lower.

The large-band boundary can be defined by the position where the fibre angle changes abruptly, consisting of both broken and unbroken kinked fibres. Small angular change in fibre direction across the narrow bands can be observed in Fig. 1a. As depicted in Fig. 5, the planes of fibre breaks are shaped differently. The upper and lower boundaries, delineating the wide band, have almost propagated across the entire specimen; while the middle planes, representing the boundaries for narrower bands, are sickle-shaped around the circumference of the rod. From the side view all the band-boundary planes were found to be inclined at around 25°, with slight bending in three dimensions. The middle fibre-fracture planes give rise to the formation of multiple narrower kink bands and the width of each kink band ranges between 25μm and 100μm.

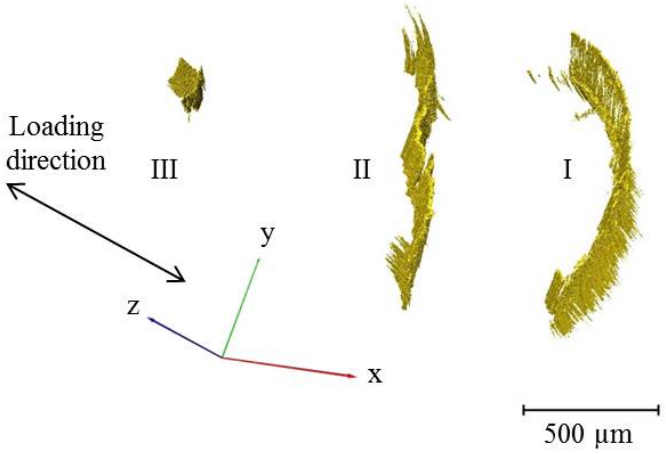

Figure 6. Top view of segmented three curved splitting planes at different locations in the specimen, numbered I, II and III.

The splits parallel to the fibre direction form curved planes in the kinked volume. The morphology of these planes changes with position along the X direction. Three typical splits were segmented near two maximum-bending surfaces and at the centre of the specimen, as shown in Fig. 4. Fig. 6 demonstrates that splits I and III are shaped as the circumference of the specimen; while the waviness of split II is because the fibre rotation angle varies in the Y direction. The morphology of the splitting planes suggests that its propagating direction is roughly along the Y axis. It can be seen in Fig. 4 that split I has stopped the propagation of fibre breakage at the lower kink-band boundary by releasing the stored strain energy.

3.2. Kink-band development

Although only post-mortem μCT qualitative analysis is conducted, damage information can be obtained from orthogonal slices at different positions along the damage propagation direction. This provides some clues as to the materials' behaviour at different stages during the loading process. In the compressive failure of laminates with high aspect ratio, due to the lack of constraint in the thickness direction, out-of-plane kink bands are dominant [4]. The specimen tested in the current study is cylindrical, with its surface unsupported, thus the lateral support is similar in all directions. Nevertheless the kink bands predominantly lie within a plane (chosen as the XZ plane) except for a few isolated parts. Specifically, the bottom small kink band highlighted in the white rectangular boxes in Fig.1a and 1b lies in the YZ plane. This could be explained as it formed first in the XZ plane and was further compressed during the propagation process after formation in the XZ plane to realign in the YZ plane.

Hapke *et al.* [3] found that only the initial band is ever found to propagate through the whole width of the specimen, and secondary bands terminate when the shared boundary with the initial bands stop. In terms of this finding, it is appropriate to consider the top and bottom narrow bands that define the points of maximum fibre deflection as the primary bands with the middle narrow bands as secondary ones caused by the sudden release of stored elastic energy. At the upper concave side, split III occurs due to tensile transverse stresses, and then reduces the lateral support of the fibres, which bend and break forming the top narrow band. At the lower convex side, fibre rotation has exceeded the maximum bending angle the fibre can bear so that fibres break and the bottom narrow band is developed. Meanwhile, at the top and bottom bands the fibres abruptly change angle from outside to the inside of the bands, whereas for the middle bands the change in fibre angle is slight. This might be explained by the band broadening mechanism of progressive addition of narrow zones of broken fibres to form a broadened band. In this case, the broadening is from both the top and the bottom towards the middle part. Nevertheless, it is not possible to determine from the post-failure image the evolution of kink bands in this experiment, which requires further verification with *in situ* observation.

4. Conclusions

In this study, kink bands have been visualised in 3-D by careful segmentation of a μCT image focusing on the boundaries of the kink-band and splitting along the fibre direction. The following conclusions are proposed:

a. Kink-band boundaries are essentially planar being inclined at around 25° with slight bending in three dimensions. The boundary planes of the narrow bands are sickle-shaped, while those of the wide band have grown across the specimen.

b. In three dimensions, splitting along the fibre direction forms curved planes, with the shape similar to the circumferences at locations near the outer layers and aligned along the rotated fibres in the middle section.
c. The morphology of multiple kink bands has been observed and two narrow bands at the top and bottom are assumed to be the initiation sites.

Acknowledgements

The authors would like to acknowledge support from the Northwest Composites Centre, the Henry Moseley X-ray Imaging Facility and the University of Manchester Aerospace Research Institute. We are also grateful to the Engineering and Physical Science Research Council (EPSRC) grants EP/F007906/1 and EP/F028431/1 for funding the Henry Moseley X-ray Imaging Facility.

References

[1] A. Jumahat, C. Soutis and A. Hodzic. A graphical method predicting the compressive strength of toughened unidirectional composite laminates. *Applied Composite Materials*, 18(1):65-83, 2011.
[2] C. R. Schultheisz and A. M. Waas. Compressive failure of composites, part I: testing and micromechanical theories. *Progress in Aerospace Sciences*, 32(1):1-42, 1996.
[3] J. Hapke, F. Gehrig, N. Huber, K. Schulte and E. T. Lilleodden. Compressive failure of UD-CFRP containing void defects: In situ SEM microanalysis. *Composites Science and Technology*, 71(9):1242-1249, 2011.
[4] M. P. F. Sutcliffe and N. A. Fleck. Microbuckle propagation in carbon fibre-epoxy composites. *Acta metallurgica et materialia*, 42(7):2219-2231, 1994.
[5] S. Sivashanker, N. A. Fleck and M. P. F. Sutcliffe. Microbuckle propagation in a unidirectional carbon fibre-epoxy matrix composite. *Acta Materialia*, 44(7):2581-2590, 1996.
[6] S. Pimenta. *Micromechanics of kink-band formation*. Master thesis, Imperial College London, 2008.
[7] P. S. Steif. A model for kinking in fiber composites—I. Fiber breakage via micro-buckling. *International journal of solids and structures*, 26(5):549-561, 1990.
[8] P. Berbinau, C. Soutis and I. A. Guz. Compressive failure of 0 unidirectional carbon-fibre-reinforced plastic (CFRP) laminates by fibre microbuckling. *Composites Science and Technology*, 59(9):1451-1455, 1999.
[9] B. W. Rosen, Mechanics of composite strengthening, in *Fiber Composite Materials*, pages 37-75. American Society for Metals: Metals Park, Ohio, 1965.
[10] A. S. Argon. Fracture of composites. *Treatise on materials science and technology*, 1:79-114, 1972.
[11] A. E. Scott, M. Mavrogordato, P. Wright, I. Sinclair and S. M. Spearing. In situ fibre fracture measurement in carbon–epoxy laminates using high resolution computed tomography. *Composites Science and Technology*, 71(12):1471-1477, 2011.
[12] G. P. McCombe, J. Rouse, R. S. Trask, P. J. Withers and I. P. Bond. X-ray damage characterisation in self-healing fibre reinforced polymers. *Composites Part A: Applied Science and Manufacturing*, 43(4):613-620, 2012.
[13] J. E. Rouse. *Characterisation of Impact Damage in Carbon Fibre Reinforced Plastics by 3D X-Ray Tomography*. EngD thesis, University of Manchester, 2012.
[14] C. W. Weaver and J. G. Williams. Deformation of a carbon-epoxy composite under hydrostatic pressure. *Journal of Materials Science*, 10(8):1323-1333, 1975.

[15] T. V. Parry and A. S. Wronski. Kinking and compressive failure in uniaxially aligned carbon fibre composite tested under superposed hydrostatic pressure. *Journal of Materials Science*, 17(3):893-900, 1982.
[16] H. Couque, C. Albertini and J. Lankford. Failure mechanisms in a unidirectional fibre-reinforced thermoplastic composite under uniaxial, in-plane biaxial and hydrostatically confined compression. *Journal of materials science letters*, 12(24):1953-1957, 1993.
[17] C. Soutis. Compression testing of pultruded carbon fibre-epoxy cylindrical rods. *Journal of Materials Science*, 35(14):3441-3446, 2000.
[18] L. A. Feldkamp, L. C. Davis and J. W. Kress. Practical cone-beam algorithm. *Journal of the Optical Society of America A*, 1(6):612-619, 1984.